Exponential life-threatening rise of the global temperature[a]

Markus Noll[b,*]

Keywords: Exponential rise of global temperature, atmospheric carbon dioxide concentration, anthropogenic CO_2 emissions, climate tipping points, consumerism vs. population growth.

[a] This is a non-peer reviewed preprint submitted to EarthArXiv. It is dedicated to the memory of my brother, Hans Noll, who early inspired my interest in molecular biology as well as climate science.

[b] Department of Molecular Life Sciences, Winterthurerstr. 190, University of Zürich, CH-8057 Zürich, Switzerland

[*] Email: markus.noll@mls.uzh.ch

Abstract

Global temperatures are rising. This paper demonstrates for the first time that the global temperature increase has not been linear but is exponential with a doubling time of about 25 years. Both the amount of carbon dioxide produced by the combustion of fossil fuels and the amount of carbon dioxide in the atmosphere have also risen exponentially, with a similar doubling time. The exponential trajectories of rising global temperature, carbon dioxide emission, and atmospheric carbon dioxide concentration support the idea that all three are entirely man-made. This analysis shows that during the past 70 years, the increasing use of fossil fuels results more from human activities than population growth, and that reducing the use of fossil fuels by 7.6% each year, the "7.6%-scenario", can prevent annual global temperatures from surpassing pre-industrial temperatures by 1.6°C, a critical threshold to sustaining life on Earth.

Introduction

Global temperature rise imperils all life on Earth. Whereas life has adapted to temperature fluctuations, our atmosphere plays a crucial role sustaining life by moderating temperature extremes such as those that would otherwise occur between day and night. For instance, Earth's daily temperature fluctuations are modest compared to temperature differences at the moon, despite the fact that the moon is on average the same distance from the sun as the Earth. The moon has essentially no atmosphere (1), and its equatorial temperatures are between +117°C in sunlight and –173°C in the dark (2). When the Earth's surface warms under the glare of sunlight, heat reflects outward in the form of infrared radiation and is captured by greenhouse gases in the atmosphere. The amount of heat the atmosphere traps is important because the trapped heat radiates back to the Earth's surface during the solar night, mitigating temperature differences between day and night (3–5). Life has adapted to the ranges of temperature that result. The problem we face is that the historical consumption of fossil fuels has increased the concentration of the predominant greenhouse gas carbon dioxide (CO_2) (5–9), and global temperatures are rising (10, 11), as first recognized by Callendar (12, 13). However, Callendar's careful analysis gained support only when Bolin and Eriksson (14), taking up studies by Revelle and Suess (15), showed that most of the CO_2 emitted by the burning of fossil fuels ended up in the atmosphere rather than the ocean. Callendar's studies were subsequently corroborated by Keeling's precise measurements across the globe, in the pristine air of the Antarctica, and on top of the Hawaiian volcano Mauna Loa (16, 17).

In 2021, the CO_2 concentration in the atmosphere was above 417 ppm, which is almost 1.5 times higher than at any time during the past 0.8 million years (18–24). It is concerning that further temperature increases will be amplified by feedback processes. For example, the increase in global temperatures accelerates the melting of the Arctic tundra permafrost, which releases increasing amounts of bacteria and archaea that produce methane, a very potent greenhouse gas, and CO_2, which in turn would result in a further temperature increase and

accelerated melting of the permafrost (25, 26). Further temperature increases will be beyond our control if they reach a global tipping point (27–33).

Some experts assert that the global average temperature must not rise more than 1.5°C above the global average temperature that existed before industrialization (27). Others insist that this goal is too ambitious and can no longer be achieved, but that we should aspire to remain below a 2°C increase over the pre-industrial temperature (29). Here I calculate the trajectory of annual global temperature increases and conclude that current plans and projected efforts to keep global temperature increases below the 1.5°C threshold are insufficient and unrealistic. I offer targets for reducing fossil fuel combustion that can achieve global 'climate neutrality' by 2048 without surpassing a threshold of 1.6°C.

Methods

Data sources

The sources for all raw data used in the analyses presented (Figs. 1–6) are indicated in the text and legends to the corresponding figures. Global temperature anomalies (Figs. 2 and 3) were taken from NASA/GISS at https://data.giss.nasa.gov/gistemp/graphs_v4/ under 'Global Annual Mean Surface Air Temperature Change'. The source for determining global CO_2 concentration anomalies (Fig. 4) till 1957 are from NASA/GISS and after 1957 from NOAA, both at https://www.sealevel.info/co2_and_ch4.html. Global CO_2 emissions (Fig. 5) from fossil fuel burning, cement manufacture, and gas flaring, reported at https://cdiac.ess-dive.lbl.gov/ftp/ndp030/global.1751_2014.ems by Tom Boden, Bob Andres, and Gregg Marland, were used till 2014, and after 2014 those at https://ourworldindata.org/co2-emissions (without land use), reported by Hannah Ritchie and Max Roser. Accumulated CO_2 emissions were computed from the annual global CO_2 emissions as described in the legend to Fig 6. The data and figure for the growth of the world's population at https://de.wikipedia.org/wiki/Datei:World-Population-Growth-1750-2100.png (Fig. 8) are from Max Roser with raw data after 1950 from elaboration of data by United Nations, Department of Economic and Social Affairs, Population Division at https://www.worldometers.info/world-population/world-population-by-year/.

Regression analysis, coefficients of determination, and confidence intervals

Nonlinear regression analysis was transformed to linear regression analysis (34, 35) by taking the logarithms of the equation for exponential functions. Best fits were obtained by the method of least squares (34, 36) and the use of standard programs, such as that available at https://keisan.casio.com/exec/system/14059930973581. These also computed the Pearson correlation coefficients (34, 37, 38) indicated in the text and figure legends. Best fits to other curves were also computed by the method of least squares (34, 36).

The square of the Pearson correlation coefficient is the coefficient of determination (34, 39). It measures the fraction of the total variation in the dependent variable, plotted on the y-axis, that is explained by the independent variable, in our case the time, plotted on the x-axis. A coefficient of determination above 80% is considered to be very good (34). In the cases reported here, the coefficient of determination for the annual global temperature anomaly is 81% (Figs. 2 and 3). This indicates that 81% of the variation of the annual global temperature anomalies since 1951 is explained by the different input values according to the exponential function of the best fit with a doubling time of 25.5±2.9 years, while the remaining 20% of the variation result from the variation of the annual global temperature anomalies that is independent of the input values of time. The coefficient of determination

for the atmospheric CO_2 concentration anomaly is larger than 99% (Fig. 4), for the annual global CO_2 emissions 95% (Fig. 5), and for the accumulated CO_2 emissions (Fig. 6) again exceeds 99%.

The standard error s of the regression parameter *k*, the growth constant, is computed as

$$s = \sqrt{\{\sum (y_i - y)^2/[(n-2)\sum (x_i - \langle x \rangle)^2]\}},$$

in which x_i is the number of years after 1950, y_i the natural logarithm of the ordinate at x_i, and y that of the best fit at x_i, while $\langle x \rangle$ is the average of all x_i and n the number of time points x_i used to determine the best fit. The standard error of *k* for Figs. 2 or 3 is calculated as 0.00158 y^{-1}. The confidence interval of *k* is determined by the *t*-value from a table of a Student's *t*-distribution with n–2 degrees of freedom, which for a 95% confidence interval, in all cases examined here, happens to be 1.99 or 2.00, with which the standard error s of *k* is multiplied. Since the doubling time T_d is inverse proportional to the growth constant *k*, the 95% confidence interval of *k* is proportional to that of T_d only for small values of the standard error of *k*, Δk, i.e., if $\Delta k \ll k$. In cases where this approximation is not accurate enough (Figs. 2, 3, and 5), the 95% confidence interval of T_d is calculated by determining its limits from the confidence interval of *k*, using the relationship $k = \ln 2/T_d$. The doubling time T_d of the best fit in these cases deviates slightly from the middle of the 95% confidence interval of T_d.

Choice of base period and baseline

The annual temperature anomalies (https://data.giss.nasa.gov/gistemp/graphs_v4/ under Global Annual Mean Surface Air Temperature Change based on Land and Ocean Data), reported by NASA/GISS and used here in Figs. 2 and 3, refer to an average temperature between 1951 and 1980 (Fig. 1), which is a standard base period used in climate science. Here, I used as baseline a temperature closer to the pre-industrial temperature by taking the average temperature between 1850 and 1920. According to NASA/GISS, which report annual temperature anomalies since 1880, the average temperature between 1880 and 1920 is 0.27°C lower than that between 1951 and 1980. To determine the reference temperature between 1850 and 1920, I used the values reported by Robert Rohde at Berkeley Earth (http://berkeleyearth.org/global-temperature-report-for-2021/), who used as reference temperature the average temperature between 1850 and 1900. Calibrating these values in the overlapping time interval between 1880 and 1920 to those of NASA/GISS, I found that the average temperature between 1850 and 1920 is 0.03°C lower than that between 1880 and 1920 in Fig. 1. Therefore, the temperature anomalies used in Figs. 2 and 3, referring to the average temperature between 1850 and 1920, are 0.30°C higher than those reported by NASA/GISS, which are depicted in Fig. 1 referring to the average temperature between 1951 and 1980. These calculations are in excellent agreement with the difference of 0.31°C between baselines used by Berkeley Earth (1850 to 1900) and NASA/GISS (1951 to 1980), computed by Berkeley Earth (http://berkeleyearth.org/global-temperature-report-for-2021/).

The chosen reference temperature, however, is important also in another respect, as it influences the doubling time inferred from the best fit obtained by regression analysis. Therefore, it is important to calculate the standard error of the reference temperature, here the average temperature between 1850 and 1920, which is used in Figs. 2 and 3 as zero line to which the annual temperature anomalies refer. This standard error, computed by using only the values of Berkeley Earth, is ± 0.015°C or, at 95% confidence, ± 0.029°C. To determine the influence this ± 0.03°C baseline error has on the doubling time of 25.1 years and the correlation coefficient of the exponential best fit in Fig. 2, the best fit was computed for a baseline 0.03°C lower and 0.03°C higher than that used in Figs. 2 and 3. Raising the baseline by 0.03°C results in a best fit with $T_{an} = 0.216\ e^{0.0258(t-1950\ y)}$°C and a doubling time of 26.9 years with a slightly enhanced correlation coefficient of 91.0%. Lowering the baseline by

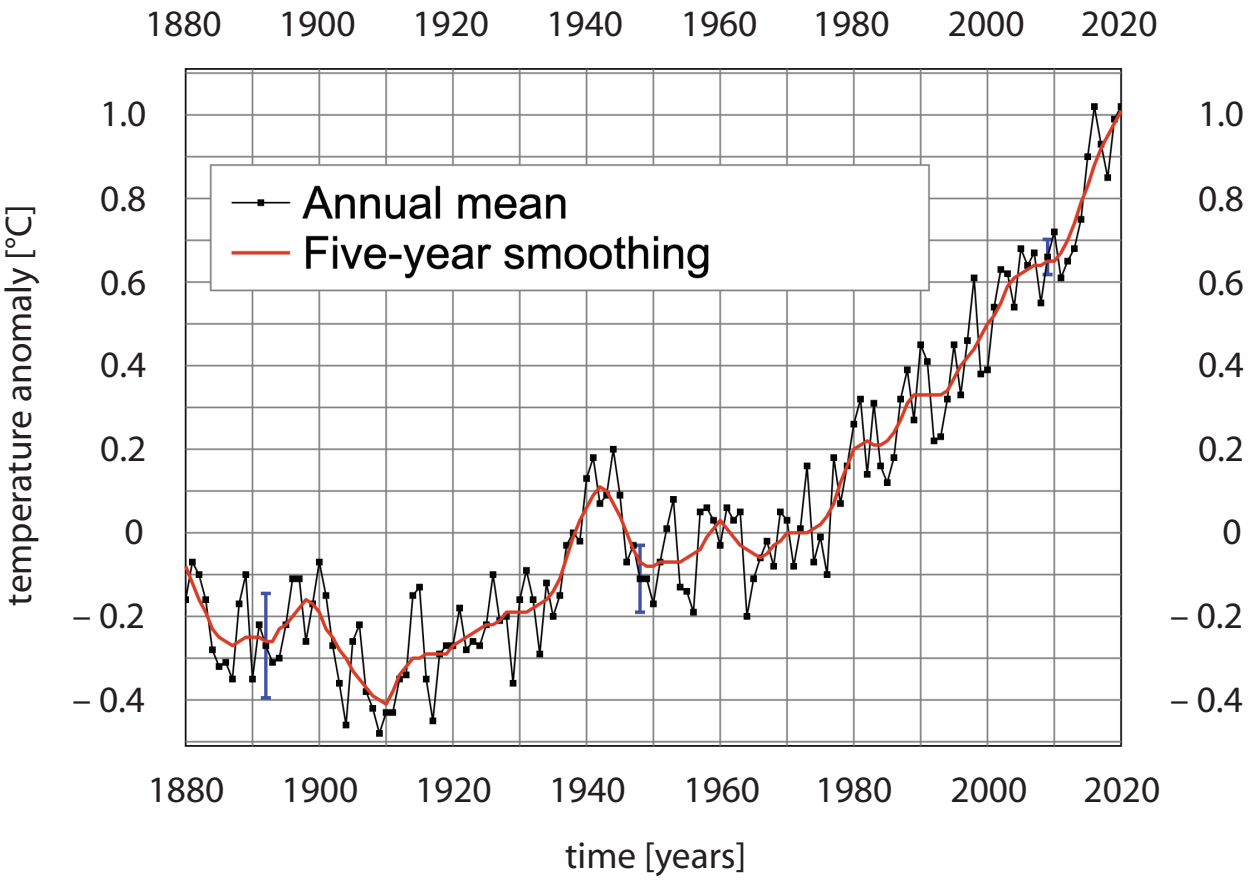

Fig 1. Rise of the global average temperature since the beginning of industrialization. The annual global average temperatures since 1880 are plotted as difference in degrees centigrade [°C] with regard to the average of the annual global temperatures between 1951 and 1980, chosen as zero line. Data (https://data.giss.nasa.gov/gistemp/graphs_v4/) from NASA/GISS for Global Annual Mean Surface Air Temperature Change, plotted at https://upload.wikimedia.org/wikipedia/commons/f/f8/Global_Temperature_Anomaly.svg.

0.03°C produces a best fit with $T_{an} = 0.162\ e^{0.0297(t-1950\ y)}$°C and a doubling time of 23.3 years with a slightly reduced correlation coefficient of 89.2%. The doubling time of the best fit to the global temperature anomaly thus has a doubling time of 25.1±1.8 years at a 95% confidence level. However, these differences in best fits for these raised or lowered baselines do not affect the prediction that the threshold of 1.5°C will be surpassed in 2025 if we continue with business as usual (Table 1). Since this baseline error of T_d is independent of its standard error determined by regression analysis, the two add up to $\sqrt{(2.9^2 + 1.8^2)}$ years = 3.4 years, thus widening the 95% confidence interval of T_d from [22.5, 28.3] years to [22.0, 28.8] years in Figs. 2 and 3.

Results

The Earth's temperature is already 1.3°C above the pre-industrial temperature

Annual global average temperatures have been recorded worldwide by instruments on land and sea since about 1850, the beginning of the industrial revolution. The plot in Fig. 1 depicts these temperatures since 1880, as reported by NASA/GISS, in relation to a convenient but arbitrary reference temperature (16, 17, 40, 41). Before 1940, global average temperatures increase and decrease but do not exceed this reference temperature. Not so after 1950 when the temperatures noticeably and steadily rise. The difference between the annual global average temperature and this reference temperature is called the 'temperature anomaly'. The reference temperature in Fig. 1 (ordinate value = 0) is calculated as the average of the annual global temperatures between 1951 and 1980, a base period frequently used as standard in climate science but well above the pre-industrial temperature, defined here as the global average temperature when the CO_2 concentration in the atmosphere began to rise noticeably, i.e., around 1850. A reference temperature closer to this pre-industrial temperature is the average of the annual global temperatures between 1850 and 1920. This reference temperature is 0.30°C below that used in Fig. 1 (41) and has a standard error of ± 0.015°C (cf. Methods). Therefore, I used this lower reference value for my analysis and conclude that the temperature anomaly today is 1.3°C above the pre-industrial temperature. This lower reference temperature fits a report in the early 1980s that the global temperature had increased by 0.4°C during the past century (8).

The global temperature anomaly increases exponentially

The temperature anomalies shown in Fig. 1 were used to calculate the curve that fits best by linear regression analysis (cf. Methods). This plot was then used to extrapolate temperatures into future years, assuming that the primary drivers of the temperature increases remain unchanged – that fossil fuels continue to be used as main source of energy. This calculation provides estimates for the years when global average temperatures are predicted to rise above the pre-industrial temperature by 1.5°C, 2.0°C, 3.0°C, and so on. Thus, the calculation provides a measure of the urgency for actions to curb global warming. The crucial question is: which curve fits the measured annual global temperature anomalies best? If the values are best fit by a linear curve, the temperature anomaly, which increases within the 40 years between 1920 and 1960 by 0.3°C (with a notable transient peak during World War II), should again increase by 0.3°C over the next 40 years. However, the values between 1960 and 2000 rise by 0.5°C, not 0.3°C.

Unlike linear curves, exponential curves have the property that equal intervals on the abscissa (time in Fig. 1) do not correspond to equal intervals on the ordinate (temperature anomaly in Fig. 1). Instead, an entity that grows exponentially doubles within the time period

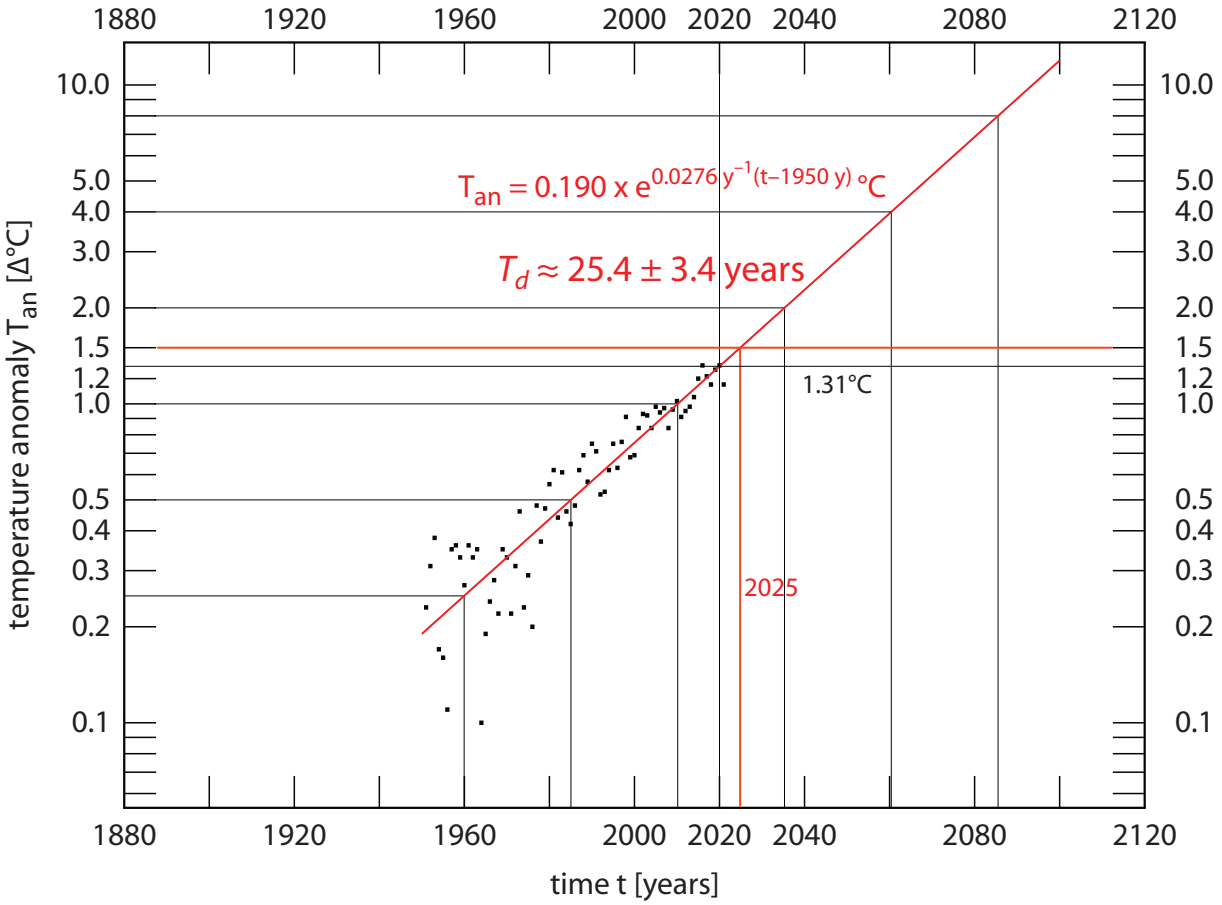

Fig. 2. The exponential rise of the global temperature anomaly has a doubling time of about 25 years. Temperature anomalies, measured as differences [Δ°C] with regard to the average temperature between1850 and 1920, which is close to the average pre-industrial temperature (cf. Methods), are plotted on a logarithmic scale as a function of time on a linear scale as semi-logarithmic plot. The best fit for time points between 1951 and 2021 (red straight line) is an exponential curve of the form $y = 0.190 \times e^{0.0276x}$ with a correlation coefficient of 90.3% (cf. Methods), in which y is the annual global temperature anomaly, T_{an}, and x the time t in years since 1950. The doubling time, T_d, characteristic of this exponential curve is computed as ln2/0.0276 years ≈ 25.1 years and can be derived from the figure: the temperature anomaly doubles five times during the 125 years between 1960 (first vertical black line), when it was 0.25°C, and 2085 (last vertical black line), when it will be 8°C. The 95% confidence interval of T_d, [22.0, 28.8] years, was determined as described in Methods. The best fit shows that 1.5°C above the pre-industrial temperature will be reached in 2025, highlighted by red horizontal and vertical lines, if we continue with business as usual. Also evident is that by the end of 2020, the temperature anomaly has reached 1.31°C, as indicated by horizontal and vertical black lines.

characteristic for the particular exponential curve, the doubling time T_d (42). Therefore, to test whether the measured annual average temperature anomaly increases exponentially with time, the values of the temperature anomaly were plotted on a logarithmic scale while keeping time on a linear scale. If the best fit to such a semi-logarithmic plot is a straight line, the increase is exponential. Fig. 2 shows a semi-logarithmic plot for the years from 1951 to 2020. Before this time period, variations of the annual average temperatures are too large to obtain a meaningful best fit because their differences to the pre-industrial temperature are too small.

The curve that best fits the values in Fig. 2 is a straight line. This line rises with a slope k that corresponds to a doubling time, T_d, of 25.1 years with a 95% confidence interval of [22.0, 28.8] years (cf. Methods). Regression analysis computes a correlation coefficient of 90% (cf. Methods). This strongly suggests that the temperature anomalies increase exponentially with a growth constant k, whereby $k = \ln 2/T_d$. These results predict that the temperature anomaly will reach 1.5°C by the end of 2025, 2.0°C by 2036±1 year, 4.0°C by 2061±3 years, and 8°C by 2086±4 years (cf. Methods). This prediction assumes that forces that propel increases in atmospheric CO_2 do not change and thus implies 'business as usual'.

The rise in global temperature does not fit a linear curve

One might argue that we can also calculate the best fit for a linear plot, as shown in Fig. 1, and compare its fit to that of the exponential plot. This is computed for the period between 1951 and 2021 and depicted in Fig. 3 as straight black line. For the years before 1964, 12/13 temperature values are above this line, whereas 12/13 are below it for the subsequent years between 1964 and 1976. Similarly, all temperature values are above the line between 2014 and 2021. This uneven distribution of the measured temperature values above and below the line of the linear best fit contrasts with the uniform distribution of the temperature values above and below the exponential best fit, depicted as red dots. Moreover, the linear best fit fails to satisfy the boundary condition approaching pre-industrial time (see below).

The rise in global temperature anomaly does not fit a quadratic or cubic curve

It could be argued that 2.8 doubling times of the exponential best fit are not enough to suggest that the temperature anomaly follows an exponential rise. Ignoring its 90% correlation coefficient, the exponential curve is strengthened by an important argument. If we assume that the cause responsible for the increasing global temperature anomaly remained the same since the onset of industrialization, as will be shown below, the best fit must also suffice the boundary condition that the global temperature anomaly is virtually 0°C at this time. This is the case for the exponential curve, which smoothly follows the annual average temperature anomalies from 1950 backwards in time to the beginning of industrialization (Fig. 3). Conversely, if the assumption is correct, it implies that warming has been exponential since the onset of industrialization. By contrast, the linear best fit does not satisfy this boundary condition. Similarly, quadratic (magenta dotted curve) and cubic best fits (blue dotted curve) that fulfill this boundary condition of 0°C global temperature anomaly at the beginning of industrialization in 1850 do not fit the temperature points as well as the exponential curve, not only but particularly during the last 30 years (Fig. 3).

The atmospheric CO_2 concentration anomaly is doubling every 29 years

Next the trajectory of the increase in atmospheric CO_2 was examined. Before industrialization, there was a balanced equilibrium between CO_2 production by organisms that use oxygen for energy production, and CO_2 removal by organisms that fix CO_2 by photosynthesis for energy production (10, 11). This fixed CO_2, which originated from organisms that lived millions of years ago, is the backbone of the fossil fuels that have been

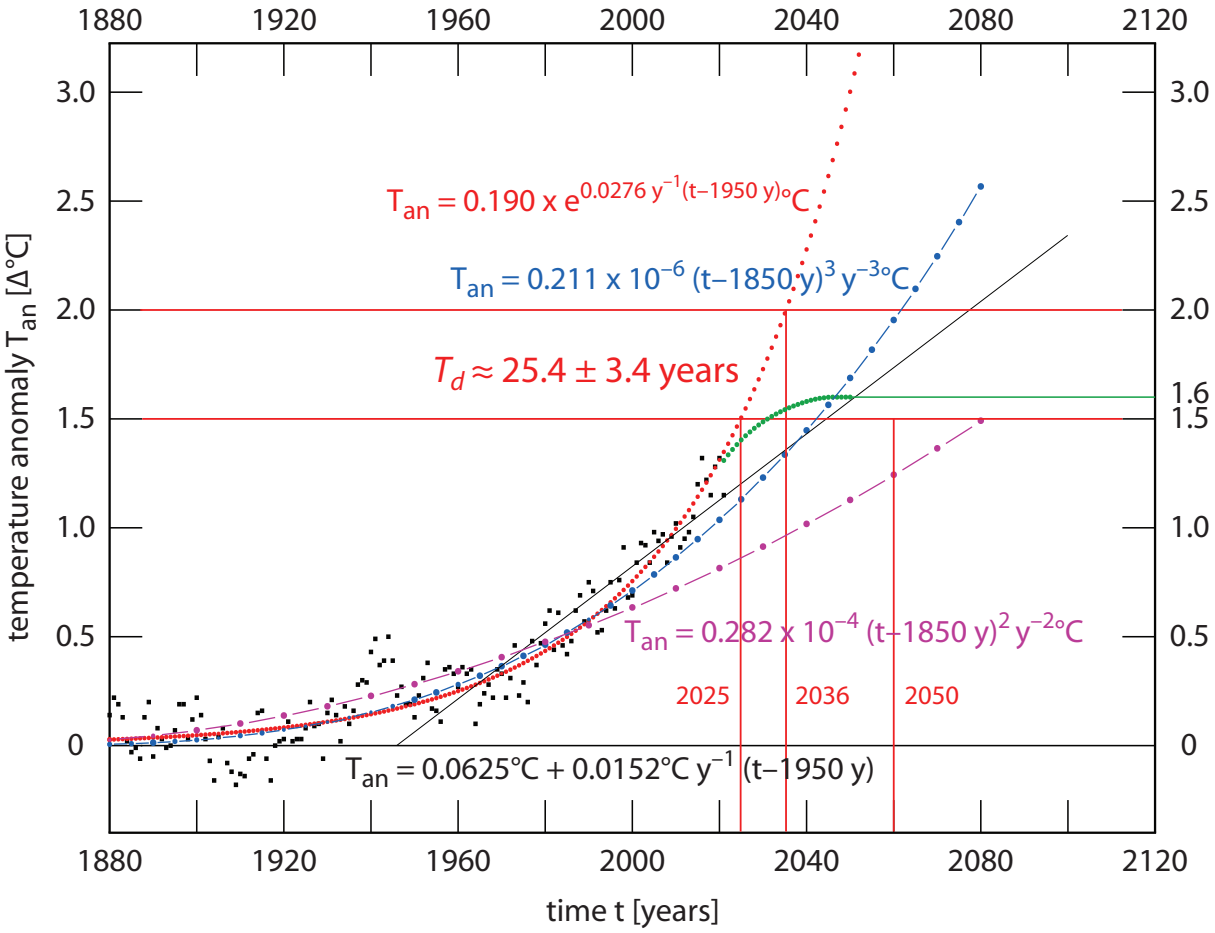

Fig. 3. Comparison favors exponential over linear, quadratic, and cubic best fits to rise of global temperature anomaly. The rise of global temperature anomaly is plotted on a linear scale as in Fig. 1. The exponential best fit for the period between 1951 and 2021 is shown as red dots of an exponential curve with the doubling time, T_d, of about 25 (ln2/0.0276) years, calculated from Fig. 2. For determining its 95% confidence interval of 25.4 ± 3.4 years cf. Methods. The linear best fit for the same period is shown as black straight line with T_{an} = 0.0625°C + 0.0152°C y^{-1} (t − 1950 y). Quadratic and cubic best fits for the same period that fulfill the boundary condition of $T_{an} \approx 0$ at t = 1850 are shown as dots in magenta and blue, respectively (cf. Methods). They do not fit the measured values of T_{an} as well as the exponential best fit. A global temperature anomaly of 1.5°C is reached in 2025 and of 2.0°C in 2036, as indicated by red lines, if we continue with business as usual. To avoid surpassing the 1.5°C threshold seems improbable. In the 7.6%-scenario, however, the temperature anomaly approaches, but does not exceed, 1.6°C, as indicated by the green dotted curve.

consumed in increasing amounts since industrialization. For at least 800,000 years before industrialization, CO_2 in the atmosphere did not exceed about 280 ppm (18–24), but the combustion of fossil fuels has upset the historical equilibrium (11), increasing CO_2 in the atmosphere to its present level above 417 ppm. Is the increase of atmospheric CO_2 concentration exponential, and if it is, what is its doubling time?

The global temperature increase was calculated relative to a global average temperature at the onset of industrialization. Similarly, the increase of atmospheric CO_2 concentration was calculated with reference to that around 1850, which was 285 ppm. By analogy to the global temperature anomaly, the atmospheric CO_2 concentration anomaly is defined as the difference in ppm, Δppm, between the annual global average of the atmospheric CO_2 concentration and that of the year 1850. To test whether the atmospheric CO_2 concentration anomalies rise exponentially, values were analyzed that had been obtained from ice cores for years prior to 1958, and values measured at Mauna Loa on Hawaii (43) for subsequent years. The CO_2 concentration anomalies and the computed best fit, for the years from 1951 to 2020, are shown in a semi-logarithmic plot in Fig. 4. Regression analysis computes as best fit a straight line with a correlation coefficient of 99% (cf. Methods), which demonstrates that the CO_2 concentration anomaly rises exponentially, with a doubling time, T_d, of 29.2±0.3 years. This doubling time is similar to the 25.4±3.4-year doubling time of the rising global temperature anomaly (Fig. 2). This result is reminiscent of the well documented cyclic correlation of atmospheric CO_2 concentrations with global temperatures over the past 800,000 years (18–24). According to Milankovitch's hypothesis, it is caused by a feedback mechanism between global temperature and atmospheric CO_2 concentration, amplifying small changes in sunlight due to orbital forcing, which results in ice ages, perduring over tens of millennia that are interrupted by shorter interglacial periods (44, 45). By contrast, the present rate of change is one to two orders of magnitude faster than what occurred during the past 800,000 years, with no end in sight. Although an exponential rise of the atmospheric CO_2 concentration between 1958 and 2000 has been implied or explicitly mentioned previously, no computation of its doubling time was shown (14, 42, 46, 47).

It is interesting to note that Fig. 4 predicts an atmospheric CO_2 concentration of 560 ppm by 2050, provided we would continue with 'business as usual'. At this time, the global temperature anomaly would reach 3.0°C (Fig. 2), which surpasses but is in fair agreement with the 2.4°C predicted for 600 ppm on the basis of sophisticated model computations by Manabe and Wetherald in 1967 (48). Moreover, it is in excellent agreement with a more recently predicted median (or equilibrium) climate sensitivity (ECS) – defined as temperature increase in response to a doubling of the atmospheric CO_2 concentration with regard to the pre-industrial time – of 2.6°C (49) and 2.8°C (50).

Is the exponential rise of the global temperature anomaly inherent or derived?

It is important to distinguish between inherent and derived exponential growth, a distinction introduced in the 30-year update of the report to the Club of Rome (47). The exponential growth is inherent if the entity considered is self-reproducing or the increment of the entity is proportional to the value of the entity. This is always true when a reinforcing feedback mechanism acts on the considered entity to increase it by a constant factor and cause it to double within a time characteristic of its growth, the doubling time T_d. In biology, a typical example of inherent exponential growth is the increase in the number of *E. coli* bacteria per volume in a liquid broth at blood heat, i.e., at the body temperature of 37°C. As long as the nutrients remain abundant and the aeration is vigorous, the bacteria double with the same doubling time, e.g., every 20 min on average, and their number increases exponentially during this so-called logarithmic or log phase. Thus, starting with one bacterium per ml, one ends up with 1.07×10^9 (2^{30}) bacteria per ml under vigorous aeration after only 30 doublings or 10

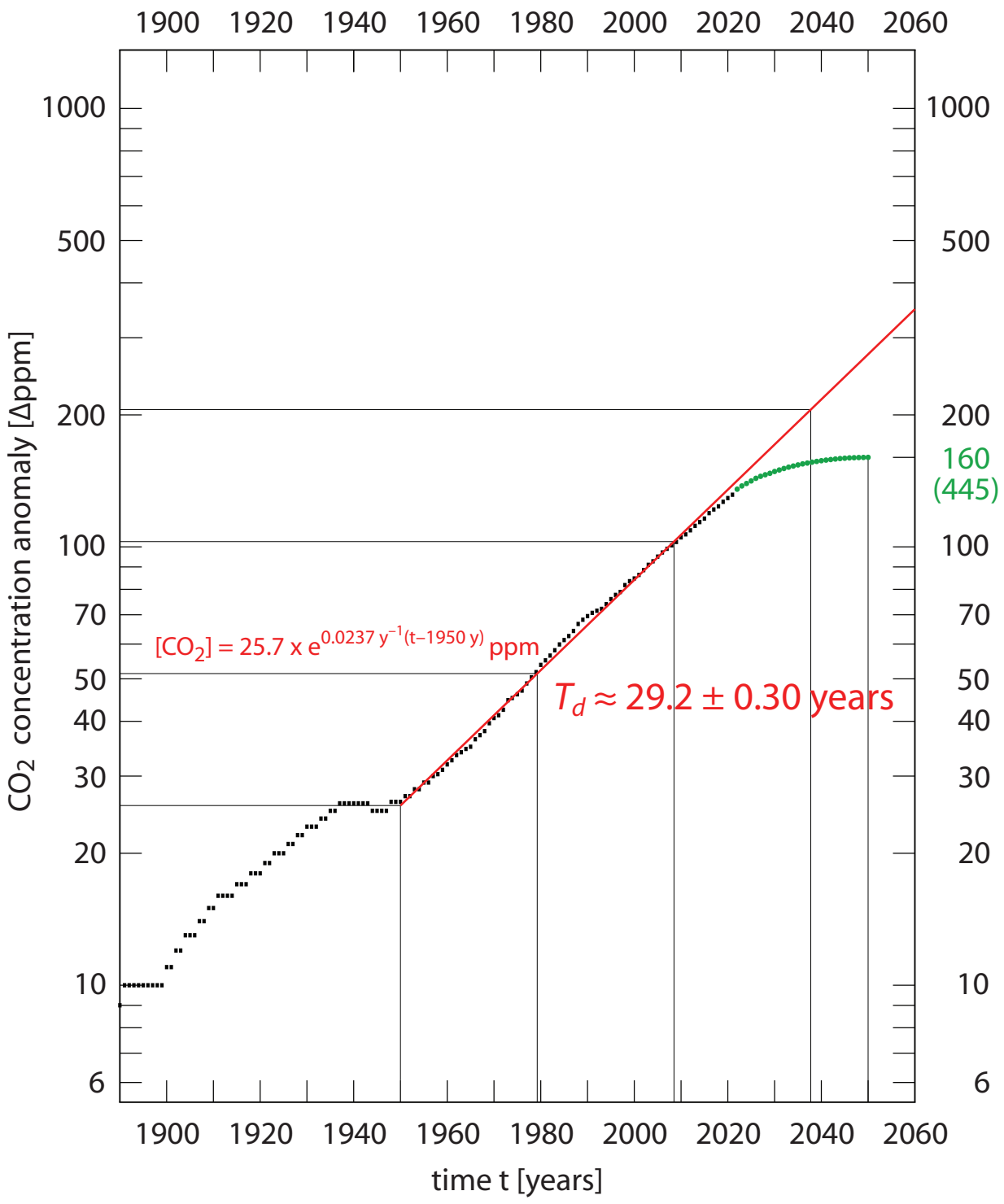

Fig. 4. Exponential rise of the atmospheric CO_2 concentration anomalies since pre-industrial times. Atmospheric CO_2 concentration anomalies are illustrated in a semi-logarithmic plot for years between 1890 and 2021. The best fit for time points between 1951 and 2021, shown as red straight line, is an exponential curve of the form $y = 25.7\ e^{0.0237x}$ with a correlation coefficient of 99.9% (cf. Methods), in which y is the CO_2 concentration anomaly and x the time in years since 1950. It has a doubling time, T_d, of ≈ 29 years, as evident from the three doubling intervals of 87.7 years between 1950 (first vertical line) and 2038 (last vertical line), during which the CO_2 concentration anomaly increases eightfold from ≈ 26 ppm to ≈ 206 ppm above the pre-industrial level. Its stadard error at a 95% confidence level is 0.30 years (cf. Methods). The CO_2 concentration anomalies are measured with regard to a reference CO_2 concentration of 285 ppm, which was constant between 1835 and 1856 and serves as pre-industrial atmospheric CO_2 concentration. It should be noted that in the 7.6%-scenario, the CO_2 concentration anomaly approaches, but does not exceed, 160 ppm above the pre-industrial concentration (green dotted curve), which corresponds to an absolute CO_2 concentration of 445 ppm. Data from NASA/GISS and NOAA/GML at https://www.sealevel.info/co2_and_ch4.html.

hours. After this log phase, bacteria will slow down in growth and doubling until they stop growing.

Derived exponential growth occurs when exponential increases are driven by another entity that is growing exponentially (47), independent of whether the exponential growth of this other entity is inherent or derived. In the following, it is argued that available evidence indicates that past increases of the global temperature anomaly are derived and dependent on human activity, the burning of fossil fuels. However, the temperature increase will become inherent if fossil fuel combustion continues to rise unabated and thus will reach a much feared global tipping point (27, 29–33).

The emission of CO_2 also rises exponentially with a similar doubling time

The similar doubling times of the global temperature anomaly (Fig. 2) and atmospheric CO_2 concentration anomaly (Fig. 4) suggest causality and the imperative to identify the drivers that increase atmospheric CO_2. Although production of CO_2 from the consumption of fossil fuel contributes CO_2 to the atmosphere, it is not a given that all of the CO_2 emissions end up in the atmosphere, or that fossil fuel combustion contributes a significant fraction to the increase of atmospheric CO_2. Most CO_2 emissions on Earth are natural and most are absorbed by sinks of the biosphere such as plants that consume and fix CO_2. Indeed, the contributions of trees to reductions of atmospheric CO_2 is the reason that logging of the tropical rainforests and boreal forests is damaging to the climate, as with the loss of trees, their capacity to remove CO_2 also disappears (11, 51–55). Nevertheless, although about 55% of human-emitted CO_2 is removed by the biosphere and the oceans at this time (56), atmospheric CO_2 concentrations have risen since the beginning of industrialization when the biosphere and oceans could not fully compensate for the increases in CO_2 emissions by industry and human activities (Fig. 4).

Again a semi-logarithmic plot tests whether the increases in annual CO_2 emissions (57) have been exponential (Fig. 5). The best fit to this plot with a correlation coefficient of 97%, computed by regression analysis for the years from 1951 to 2014, is a straight line (red line in Fig. 5), which shows that the annual CO_2 emissions have also followed an exponential growth curve with a doubling time, T_d, of 27.5±1.6 years at a confidence level of 95% (cf. Methods). However, in recent years (58), since 2015, emissions appeared to stabilize at 35.8±0.30 Gt (Gigatons), which will be discussed below. A similar effect, though not as striking, might be observed in a slightly reduced rise of the atmospheric CO_2 concentration since 2015 (Fig. 4).

The rise of the global temperature anomaly is derived and man-made

This doubling time of 27.5±1.6 years for CO_2 emissions is again similar to the 25.4±3.4-year doubling time of the exponential rise in global temperature anomaly (Fig. 2) as well as to the 29.2±0.30-year doubling time of the exponential rise in CO_2 concentration anomaly (Fig. 4). This suggests that the exponential increase in the global temperature anomaly is not yet inherent, but derived from the exponential increase of industrial CO_2 emissions as a consequence of the increasing historical combustion of fossil energies in the past. In other words, a global tipping point is not yet reached. It also confirms impressively that the increasing global temperature is man-made and hence can be stopped, provided the necessary actions are taken. This is the good news. The bad news is that if fossil fuel use continues unabated, global temperature anomalies of 2.0°C will be reached by 2036±1 year, 4.0°C by 2061±3 years, and 8°C by 2086±4 years (Fig. 2 and Methods). Therefore, actions to reduce CO_2 emissions are extremely urgent.

We have seen now that the increase in global temperature anomaly is exponential and occurs in parallel to the exponential increase of global combustion of fossil fuels. Both

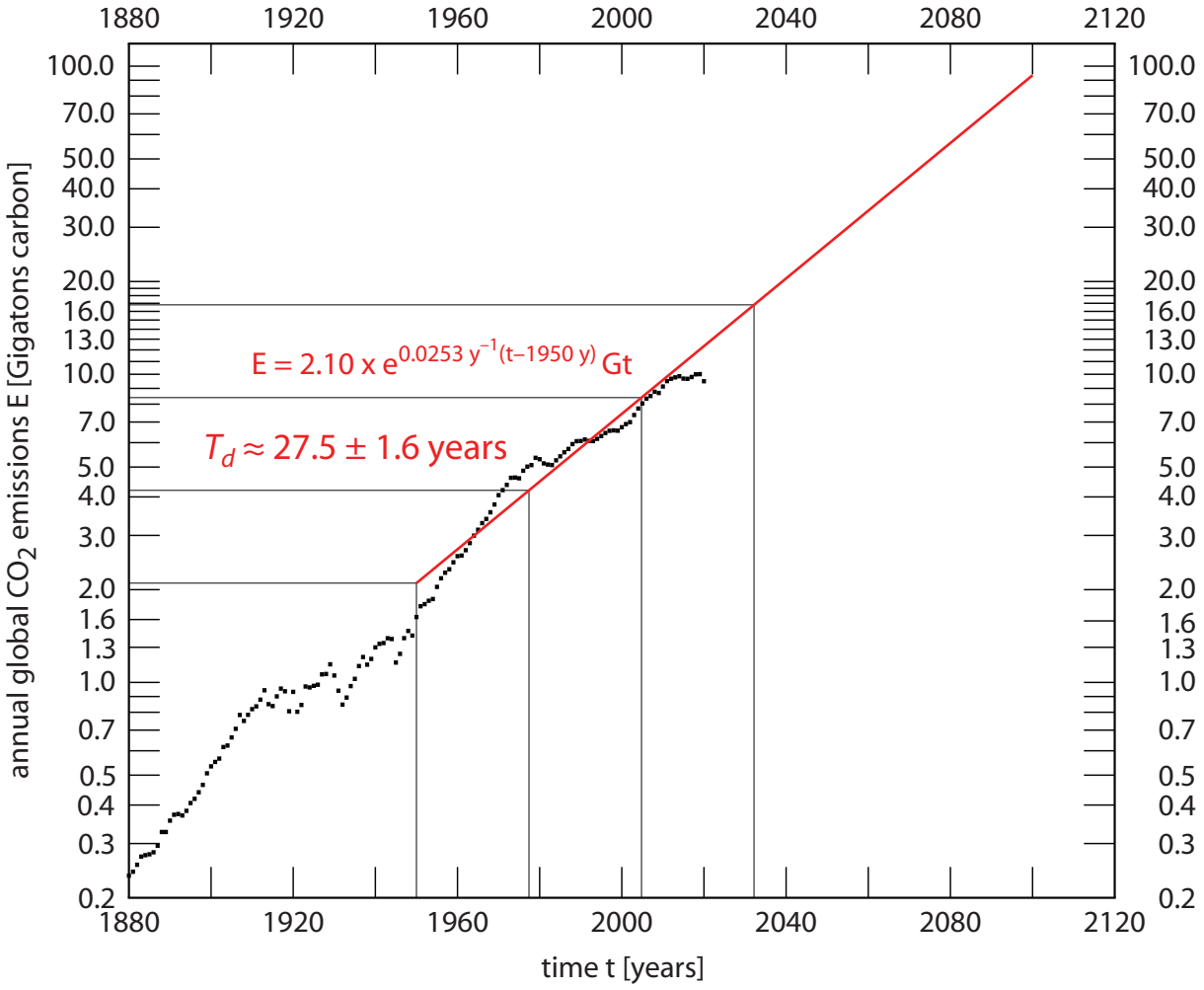

Fig. 5. Global CO_2 emissions also follow an exponential curve, doubling every 27.5 years. Annual global emissions of CO_2 are shown in a semi-logarithmic plot for years between 1880 and 2020. The best fit for the years between 1951 and 2014, shown as red straight line, is an exponential curve of the form $y = 2.10\ e^{0.0253x}$ with a correlation coefficient of 97.4% (cf. Methods), in which y is the annual CO_2 emission, E, in Gt carbon and x the time in years since 1950. It has a doubling time, T_d, of 27.4 (ln2/0.0253) years, as evident from the three doubling intervals of 82 years between 1950 (first vertical line) and 2032 (last vertical line) during which the annual CO_2 emission increases eightfold from 2.1 Gt to 16.8 Gt carbon. The 95% confidence interval of [25.9, 29.1] years was determined as described in Methods. When emissions after 2014 were included in the regression analysis, the doubling time was raised to 28.6 years. Emissions are indicated in Gigatons (Gt) carbon per year, which would have to be multiplied by 3.667, if they were given in metric tons of CO_2, as is also frequently done. Emissions between 1880 and 2014 were from https://cdiac.ess-dive.lbl.gov/ftp/ndp030/global.1751_2014.ems, and after 2014 from https://ourworldindata.org/co2-emissions (without land use).

exponential curves have doubling times that are within limits of error the same. In addition, both are not inherently exponential: the exponential increase of the global temperature anomaly is derived from the exponentially increasing CO_2 emissions by burning of fossil fuels. The exponential emissions, in turn, are not systemically inherent either, but derived, as they depend on human behavior and hence on the exponential growth of the human population and on the exponential increase of consumption of fossil energies caused to a large extent by our consumerism (14, 15, 42, 46, 59).

Accumulated CO_2 emission and global temperature anomaly rise in parallel

Because the annual average temperature anomalies and the annual emissions of CO_2 rise with the same doubling time, as shown in Figs. 2 and 5, one might surmise that the rise in CO_2 emissions cause the rise of the temperature anomalies, as argued above. However, their correlation is more complicated as evident from the following considerations. Let us assume that no further increases in annual CO_2 emissions occur and that they remain constant at the present level of about 36 Gt CO_2 (without land use). To find out how the global temperature anomaly will behave in this scenario, we must consult Table 1. It lists global temperature anomalies (column 2), atmospheric CO_2 concentrations (columns 5 and 6), and CO_2 emissions (column 3), as predicted from the best fits in Figs. 2, 4, and 5. Most important, Table 1 lists the amount of CO_2 that accumulates since 2015 (column 4) at the time when a certain global temperature anomaly is reached (column 2). Thus, by the end of 2025, 1.50°C will be surpassed which corresponds to the accumulation of 489 Gt of CO_2. A simple calculation shows that to avoid surpassing 1.50°C above pre-industrial temperatures, only 237 Gt of CO_2 may be emitted, starting with the year 2022. This follows from the fact that at the end of 2021, the budget was 489 Gt of CO_2 minus what has been emitted after 2014, which is 252 Gt CO_2 (last column in Table 1), and thus equals 237 Gt of CO_2 to stay below the threshold of 1.50°C. This budget is independent of the path by which it is reached. As long as it is not exceeded, the temperature anomaly will not surpass 1.5°C. However, these calculations suggest that the expectation to be able to keep the global temperature below 1.5°C above pre-industrial levels is unrealistic. Therefore, we should aim to avoid surpassing 1.6°C (see below).

Table 1 now permits us to answer the question of how the global temperature anomaly will behave if annual emissions of CO_2 remain constant. For example, if CO_2 continues to be emitted at 36 Gt per year, as during the past seven years from 2015 to 2021, 180 Gt were emitted by the end of 2019, 360 Gt will be emitted by the end of 2024, 540 Gt by the end of 2029, 720 Gt by the end of 2034, and so on. As evident by interpolation between the values shown in Table 1, at 180 Gt of accumulated CO_2 emissions, the global temperature anomaly has reached 1.25°C, at 360 Gt it will reach 1.39°C, at 540 Gt 1.54°C, and at 720 Gt 1.68°C, and so on. It is easy to see that in each 10-year period, the temperature will rise by the constant value of 0.29°C. In other words, the global temperature anomaly will increase linearly with time by 0.029°C per year if the annual emission of CO_2 remains constant at 36 Gt CO_2. In this scenario, 1.5°C will be surpassed in 2028 and 2.0°C will be reached by 2045.

Of course, the *accumulated* CO_2 emission will also increase linearly with time, as we have kept the annual CO_2 emission constant. Therefore, in this case it is the *accumulated* CO_2 emission that parallels the rise of the global temperature anomaly. This conclusion is entirely consistent with predictions from climate models that include climate–carbon feedbacks (60, 61).

As we have seen, when the annual emission of CO_2 rises exponentially, the global temperature anomaly also rises exponentially with a similar doubling time. In addition, the *accumulated* CO_2 emissions also rise exponentially, as evident from a semi-logarithmic plot (Fig. 6). The plotted values were determined by adding the annual emissions (Fig. 5) to the

Table 1. Predicted rise in global temperature, CO_2 emission, and atmospheric CO_2 concentration for scenarios with 'business as usual', and 7.6%-scenario keeping the temperature anomaly below 1.6°C.

	scenario with 'business as usual'					7.6%-scenario to stay below 1.6°C temperature anomaly	
		global CO_2 emission [Gigatons]		atmospheric CO_2 concentration [ppm]		global CO_2 emission [Gigatons]	
year	global temperature anomaly [°C][1)]	per year[2)]	accumulated[3)]	ΔCO_2[4)]	total CO_2	per year[5)]	accumulated[6)]
2015	1.14	39.9	40	116 (120)	401	(36)	
2016	1.17	40.9	81	119 (123)	404	(35)	
2017	1.21	41.9	123	122 (126)	407	(36)	
2018	1.24	43.0	166	124 (129)	409	(37)	
2019	1.28	44.1	210	127 (132)	412	(37)	
2020	1.31	45.3	255	129 (135)	414	(35)	
2021	1.35	46.4	302	132 (138)	417	36	(252)
2022	1.39	47.6	349	142	427	33.3	285
2023	1.42	48.8	398	145	430	30.7	316
2024	1.46	50.1	448	148	433	28.4	344
2025	1.51	51.4	499	152	437	26.2	371
2026	1.55	52.7	552	156	442	24.2	395
2027	1.59	54.0	606	159	444	22.4	417
2028	1.64	55.4	662	163	448	20.7	438
2029	1.68	56.8	718	167	452	19.1	457
2030	1.73	58.3	777	171	456	17.7	475
2031	1.78	59.8	836	175	460	16.3	491
2032	1.83	61.3	898	179	464	15.1	506
2033	1.88	62.9	961	184	469	13.9	520
2034	1.93	64.5	1,025	188	473	12.9	533
2035	1.98	66.1	1,091	193	478	11.9	545
2036	2.04	67.8	1,159	197	482	11.0	556
2037	2.10	69.6	1,229	202	487	10.2	566
2038	2.16	71.4	1,300	207	492	9.4	575
2039	2.22	73.2	1,373	212	497	8.7	584
2040	2.28	75.1	1,448	217	502	8.0	592
2041	2.34	77.0	1,525	222	507	6.9	599
2042	2.41	79.0	1,604	227	512	5.8	605
2043	2.47	81.0	1,685	233	518	4.7	610
2044	2.54	83.0	1,768	238	523	3.6	613
2045	2.62	85.2	1,854	244	529	2.5	616
2046	2.69	87.4	1,941	250	535	1.4	617
2047	2.76	89.6	2,031	256	541	0.3	617
2048	2.84	91.9	2,122	262	547	0	617
2049	2.92	94.2	2,217	268	553	0	617
2050	3.00	96.7	2,313	275	560	0	617

[1)] Values from best fit in Fig. 2. [2)] Values from best fit in Fig. 5 but in Gt CO_2 rather than carbon. [3)] Accumulated annual emissions since 2015 listed in column 3. [4)] Values from best fit in Fig. 4, except for years 2015–2021 where measured data from Fig. 4 were used (values for best fit in parentheses). [5)] Values in parentheses (2015–2020) are measured data, as opposed to those in column 3, which are derived from the best fit. The 36 Gt CO_2 in 2021 is an educated guess. After 2021, annual global emissions are calculated according to the 7.6%-scenario. [6)] Value in parenthesis represents for 2021 the measured accumulated global emission since 2015, as opposed to 302 Gt CO_2 from best fit in column 4.

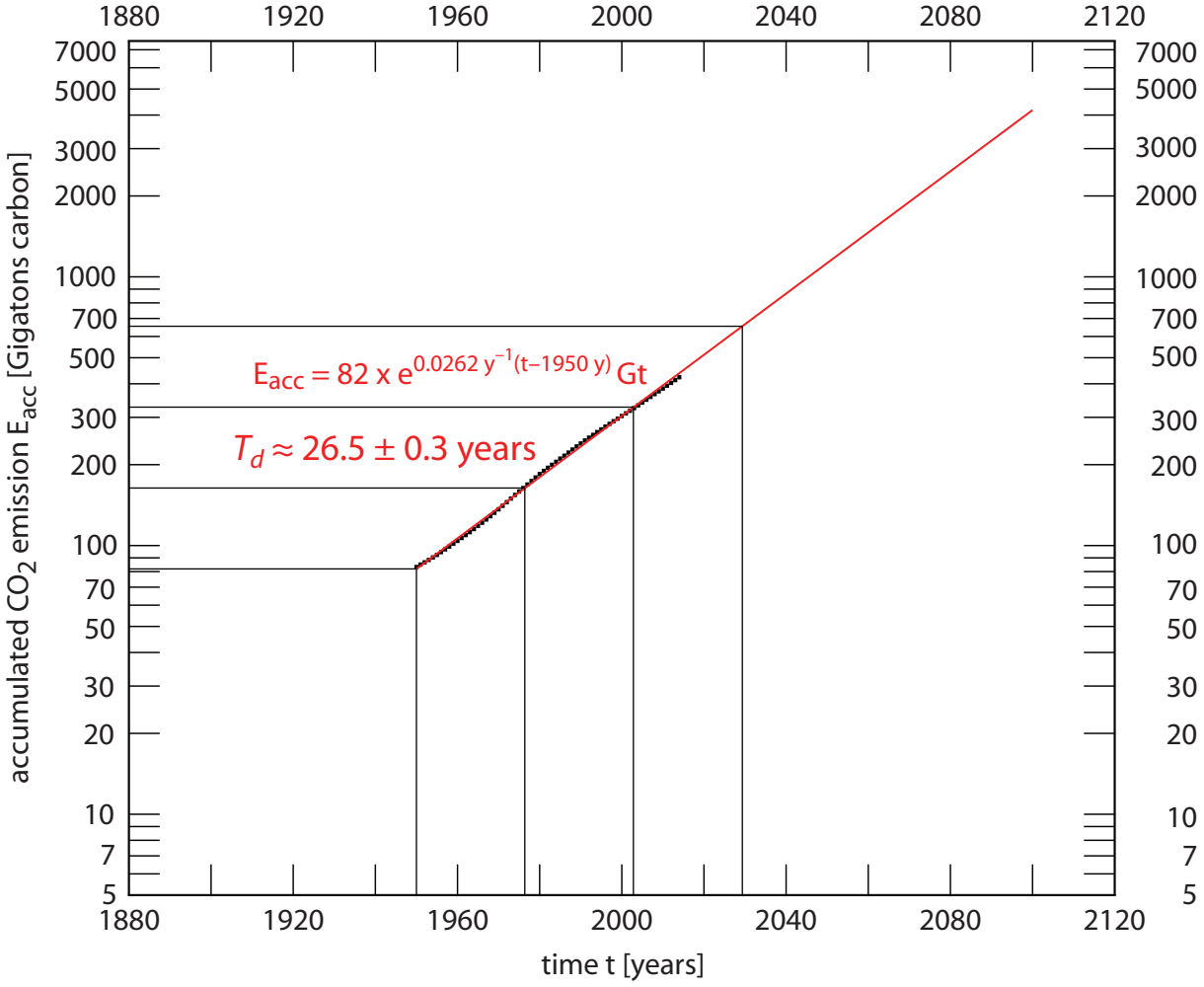

Fig. 6. Accumulated global CO_2 emission also follows an exponential curve, doubling every 27 years. The accumulated global emission of CO_2, E_{acc}, is shown in a semi-logarithmic plot between 1951 and 2014. The accumulated emission for 1950 was obtained by integration of the best fit to the annual global CO_2 emissions in Fig. 5, resulting in $y = (2.10/0.0253)\ e^{0.0253x}$. Setting $x = 0$ at 1950, this amounts to 83 Gt of carbon. To this value, annual global emissions (Fig. 5), were added to yield the accumulated CO_2 emissions. The best fit, shown as red straight line, is an exponential curve of the form $y = 82\ e^{0.0262x}$ with a correlation coefficient of 99.9% (cf. Methods), in which y is the accumulated CO_2 emission in Gt carbon and x the time in years since 1950. It has a doubling time, T_d, of 26.5 years (ln2/0.0262), as evident from the three doublings of the accumulated emission between 1950 and 2029, the first and last vertical lines. Its standard error at a 95% confidence level is 0.28 years.

total emission accumulated by 1950, obtained by integration of the best fit to the annual emissions of CO_2 (Fig. 5). The best fit to the plot in Fig. 6 with a correlation coefficient of 99%, computed by regression analysis for the years from 1951 to 2014, is a straight line with a characteristic doubling time, T_d, of 26.5±0.3 years at a 95% confidence level (cf. Methods), which, as expected, is not significantly different from the 27.5±1.6-year doubling time of the annual emissions of CO_2 (Fig. 5).

Most important, the conclusion seems inevitable that annual global temperature anomaly, accumulated global emission of CO_2, and annual atmospheric CO_2 concentration anomaly have all risen exponentially with similar doubling times, which suggests that CO_2 emission due to the combustion of fossil fuels is at the origin of the others.

What is necessary to keep the global temperature anomaly below 1.6°C?

To be able to answer this critical question, we consult again Table 1, which lists predictions made under the assumption that humanity continues with 'business as usual'. It shows that 1.60°C above the pre-industrial temperature is reached in 2028 when about 617 Gt of CO_2 will have been emitted since the beginning of 2015 if annual global temperatures continue to rise on the path of the best fit shown in Figs. 2 and 3. In other words, if global temperatures are not to surpass 1.6°C above the pre-industrial temperature, a global budget of about 617 Gt of CO_2 emissions, starting in 2015, or 365 Gt at the beginning of 2022 (617 Gt – 252 Gt; Table 1), must not be exceeded.

Table 1 permits us to test the validity of strategies proposed to keep the global temperature anomaly below a certain critical limit. All we need to do is to calculate how much CO_2 is emitted by the strategy during the period proposed to achieve climate neutrality and compare it to the remaining budged of CO_2. A recent strategy, proposed to fulfill the 1.5°C limit and achieve the goal of climate neutrality, consisted in an annual reduction of global CO_2 emissions by 7.6% (62), for simplicity called here the 7.6%-scenario. However, as shown here, in the meantime such a scenario appears unrealistic to avoid this threshold. Therefore, the 7.6%-scenario outlined below is designed not to surpass a 1.6°C threshold.

It is easy to calculate the annual global CO_2 emissions for such a scenario. Let us assume the annual emissions are reduced by 7.6% in 2022 and subsequent years. The results of these calculations are shown for each year in the two right-most columns of Table 1. In 2022, the annual emission would be 36 Gt (the estimated annual global emission in 2021) times 0.924, in 2023 36 Gt x $(0.924)^2$, in 2024 36 Gt x $(0.924)^3$, and so on. The resulting emissions reduced in this manner and the accumulated emissions since the beginning of 2015 in Gt are listed in the two right-most columns of Table 1. By the end of 2040, 592 Gt of the 617 Gt budget will be used up (Table 1). The budget of 25 Gt remaining at the end of 2040 will then be reduced in a linear fashion to reach climate neutrality by 2048 (Table 1). This scenario is also illustrated graphically in Fig. 7. It shows the annual CO_2 emissions as percentage of the emission in 2021 for every year thereafter (green dots). In this 7.6%-scenario, the global temperature and the atmospheric CO_2 concentration approach 1.6°C and 160 ppm above pre-industrial levels (dotted green curves in Figs. 3 and 4, respectively).

How to assess the effectiveness of other scenarios

To remain below the critical 1.6°C limit by the time climate neutrality is achieved, the 7.6%-scenario would just do it. The reduced annual emissions in this scenario form a geometric series of 20 members with the non-reduced emission of 2021 being its first member a_0. Therefore, its accumulated emissions, to be compared with the CO_2 emission budget, is simply calculated as the sum S_n of a geometric series as $S_n = a_0 (1–q^n)/(1–q)$ where q is the factor of the geometric series, which in the 7.6%-scenario is 0.924, and a_0 is 36 Gt (Table 1).

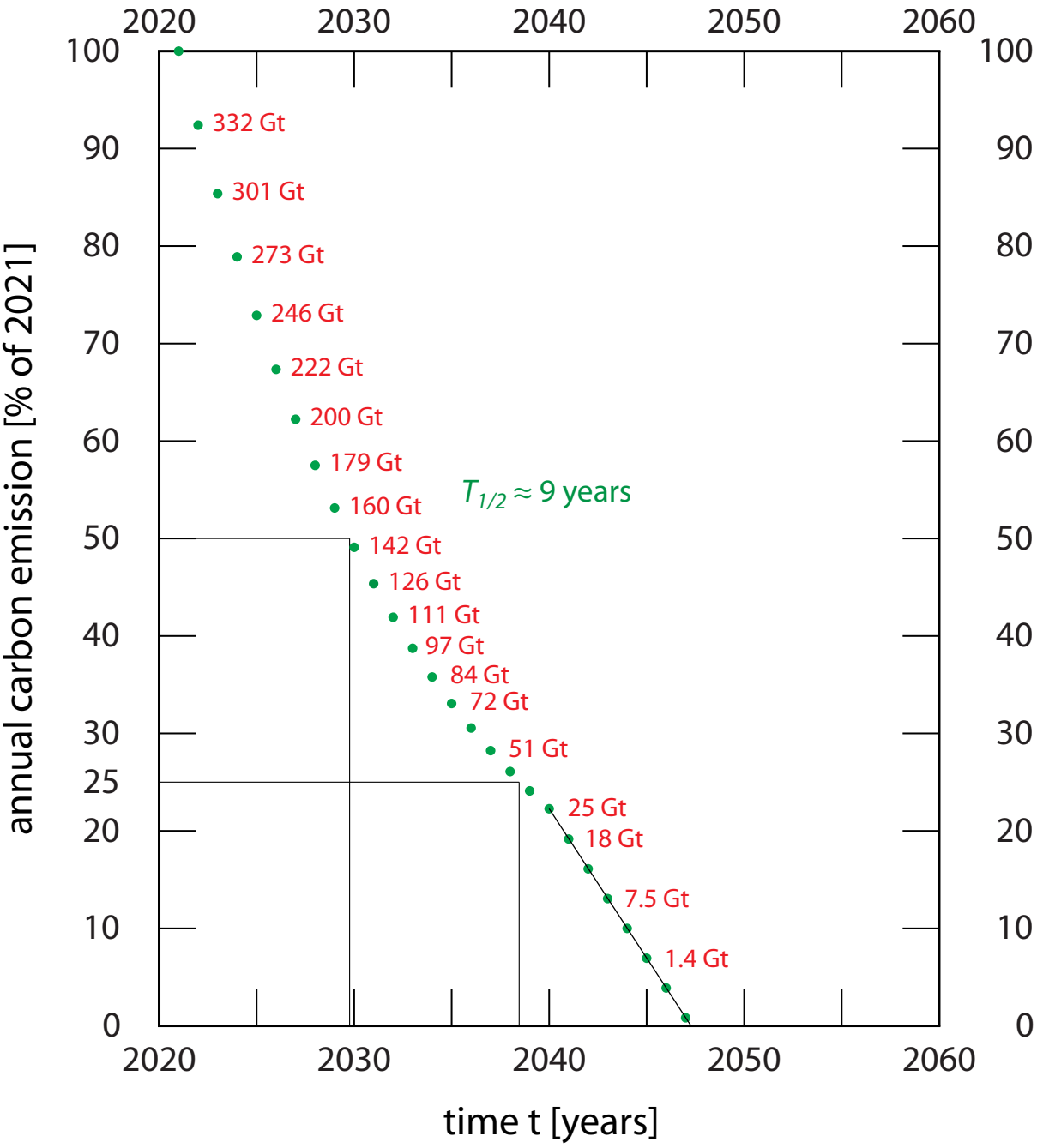

Fig. 7. **The 7.6%-scenario achieves climate neutrality without exceeding the 1.6°C temperature limit.** This scenario illustrates another type of exponential curve (green dots between 2021 and 2040), that of an exponential decay, which is characterized by an exponential decay constant or negative growth constant of 7.6% per year: $y = e^{-0.076(x-2021)}$, in which y is the fraction of annual carbon emission in 2021 and x the time in years (as the exponential decay equation holds for continuous rather than discrete time values, the exact decay is given by the geometric series between 2021 and 2040 in Table 1). While the exponential growth constant is linked to the doubling time, T_d, the exponential decay constant is linked by the same relationship to the half-life, $T_{1/2}$, during which the values are halved. Accordingly, the half-life of the 7.6%-scenario is calculated by dividing 0.693 (or ln2) by the decay constant, here 0.076 per year, which equals about 9 years, as verified by Table 1 and indicated by the vertical lines when the 36 Gt of CO_2 emission assumed for 2021 (Table 1) are reduced to 50% in 2030 and to 25% in 2039. Hence, the efficiency of a scenario can be estimated very quickly from its half-life, derived from its rate of annual CO_2 reduction. The red numbers next to the green dots indicate the remaining CO_2 budget, which, in this scenario, will be reduced to 25 Gt by the end of 2040, when the annual global emission of CO_2 will be reduced to 8.0 Gt (Table 1). A further constant annual reduction of the global CO_2 emission by about 1.1 Gt will reduce it to 0 by 2048, indicated also by a green dotted, but linear curve (shown as straight line).

Thus, if we wish to assess the effectiveness of alternative, less demanding reduction scenarios forming a geometric series, for example a 5%-scenario, we find by the end of 2040 (with q = 0.95, n = 20, and a_0 = 36 Gt) S_{20} = 462 Gt. Therefore, the total accumulated emission after 2014 is 216 Gt + 462 Gt = 678 Gt, surpassing our budget of 617 Gt and the 1.6°C already by the end of 2040 (Table 1), while the annual emission has been reduced in 2040 to 8.0 Gt. To avoid surpassing the 1.6°C limit, we could end the 5%-scenario five years earlier at the end of 2035. In this case, the accumulated emission from the beginning of 2015 to the end of 2036 will be 216 Gt + 386 Gt = 602 Gt, with a remaining budget of 15 Gt, while the annual emission has been reduced in 2035 to 11.9 Gt CO_2. Using this scenario, one might achieve climate neutrality by 2040 if the emissions are reduced to 8, 4, 2, 1, and 0 Gt CO_2 in subsequent years.

A delay in reducing the use of fossil energies has drastic consequences and will compromise any future scenario as argued above. Should annual global emissions of CO_2 remain constant, as during the period from 2015 to 2021, the global temperature will rise at a rate of 0.29°C per decade. For example, another five years of constant annual emissions of 36 Gt CO_2 would halve the remaining budget from 365 Gt to a mere 185 Gt, virtually rendering it impossible to avoid surpassing the 1.6°C threshold. Each year delaying the 7.6%-scenario reduces not only the remaining budget by 10% but also the time left to reduce the emissions to achieve climate neutrality while not surpassing the 1.6°C threshold.

Comparison with conclusions of most recent IPCC report

A given amount of accumulated global CO_2 emissions results in a distinct global temperature anomaly, independent of the path by which this temperature is reached. It follows that the limit not to be surpassed by a certain global temperature anomaly, say 1.5°C, has a cognate carbon budget of accumulated CO_2 emissions (since the end of 2014; columns 2 and 4 in Table 1). The most recent IPCC report of 2022 estimates a remaining CO_2 budget of 500 Gt since the end of 2019 for limiting the global temperature anomaly to stay below 1.5°C with a 50% probability, and a budget of 1,150 Gt for limiting the global temperature anomaly to below 2°C with a 67% probability (63). These predictions outdate an earlier IPCC report in which a remaining budget of about 420 Gt CO_2 for a two-thirds chance of limiting warming to 1.5°C, and of about 580 Gt CO_2 for an even chance (64). In this earlier report the remaining carbon budget is defined as cumulative CO_2 emissions from the start of 2018. Astonishingly, the older report is closer to my predictions as we shall see.

Table 1 predicts a remaining carbon budget since the end of 2019 of only 308 Gt for remaining below 1.5°C, namely 489 Gt (at 1.50°C) minus 181 Gt that has been accumulated between the end of 2014 and 2019 (second last column in Table 1). Indeed, according to Table 1, at the end of 2021 the carbon budget for staying below 1.5°C had been further reduced to a mere 237 Gt (489 Gt – 252 Gt), less than half of the carbon budget reported by the IPCC (63). Conversely, the accumulation of 500 Gt of CO_2 since the end of 2019, suggested by the IPCC to limit the global temperature anomaly to 1.50°C with a 50% probability, results in a global temperature anomaly of 1.65°C, corresponding to 500 Gt + 181 Gt = 681 Gt of accumulated CO_2 (Table 1). Similarly, we can calculate the temperature anomaly reached after CO_2 emissions have accumulated 1,150 Gt since the end of 2019, a carbon budget for remaining below 2°C with a 67% probability according to the IPCC report (63). From Table 1, we obtain for 1,150 Gt + 181 Gt = 1,331 Gt accumulated global CO_2 emissions (since the end of 2014) a global temperature anomaly of 2.19°C, a value well above 2.0°C.

Above we have calculated what would happen if we continued to emit globally 36 Gt of CO_2 per year as during the past seven years (Fig. 5 and Table 1). When would we surpass 1.5°C, 2.0°C, and 2.5°C under these conditions? For 1.5°C, the remaining CO_2 budget is 237

Gt CO_2, which suggests that the budget is surpassed in 2028, as pointed out above. For 2.0°C, the remaining budget since the end of 2021 is 1,114 Gt CO_2 (Table 1) and thus this temperature would be surpassed in 24 years, i.e., by the end of 2045, as calculated above. For 2.5°C, the remaining budget (since the end of 2021) is 1,721 Gt – 252 Gt = 1,469 Gt CO_2 (Table 1) and thus this temperature would be surpassed in 1,469/36 years, i.e., by the end of 2062.

As emphasized, these calculations reflect the case in which we continue on the road since 2014, emitting annually a constant vale of 36 Gt of CO_2. These calculations further illustrate that the temperature anomaly is rising linearly when the *accumulated* emissions of CO_2 also rise linearly, i.e., the annual emissions remain constant. The difference between 2045 (2.0°C) and 2028 (1.5°C) is 17 years, as it is between 2062 (2.5°C) and 2045 (2.0°C).

Not surprisingly, my predictions are more stringent than even the most recent predictions of the IPCC, since the latter continues to assume that the global temperature anomaly rises linearly rather than exponentially with time (63). For the same reason, my computation that the global temperature anomaly has already reached 1.3°C (Fig. 2) is also significantly higher than 1.1°C or 1.2°C, most frequently reported. I wish to emphasize that these differences do not occur because the pre-industrial global temperature, with regard to which the global temperature anomalies have been plotted in Fig. 2, is defined as average global temperature between 1850 and 1920, whereas the global temperature anomalies given by NASA/GISS in Fig. 1 refer to the average global temperature between 1951 and 1980. As has been carefully explained in Methods, the temperature differences amount only to 0.03°C.

My conclusions are in line with those of a recent report (65) but have the great advantage that their basis can be understood easily by all scientist without having to rely on results obtained by the use of sophisticated computer programs many of the parameters of which are uncertain.

The excessive use of fossil energies today results more from human activities than population growth

As shown above, the global temperature anomaly is on a trajectory that will increase to 1.5°C by 2025, to 2.0°C by 2036, and to 3.0°C by 2050 if we continue with business as usual (Fig. 2). As mentioned above, during this period of dramatically increasing global temperatures, a global tipping point in the Earth system of an inherent temperature increase and a runaway situation might be reached in which human activity cannot mitigate further increases in global temperature (27, 29–33). To avoid such a situation, let us examine the use of fossil energies responsible for the exponential increase in the global temperature anomaly. We can divide this increase into two components, an increase of the world's population and an increase of the average consumption of fossil energies per person, the product of which represents the total increase of fossil energy use. This product has been increasing exponentially with a constant doubling time of 27.5 years (Fig. 5), which corresponds to a growth constant k of about 2.5% per year, namely ln2/(27.5 years). This growth constant in turn is the sum of two constants that characterize the exponential growth of its two components, the world's population and the average consumption of fossil energies per person. However, whereas the total consumption of fossil energies has been increasing with a growth constant of 2.5% per year, which remained constant (Fig. 5), the growth 'constants' of its two components are not constant but have both changed since the beginning of industrialization. Yet their growth 'constants' add up to the growth constant of the global use of fossil energies, which follows from the fact that the product of two exponential functions is an exponential function whose growth constant k is the sum of the growth constants, $k_1 + k_2$, of each exponential function. Therefore, we can calculate from the growth constant of 2.5% per year of the use of fossil

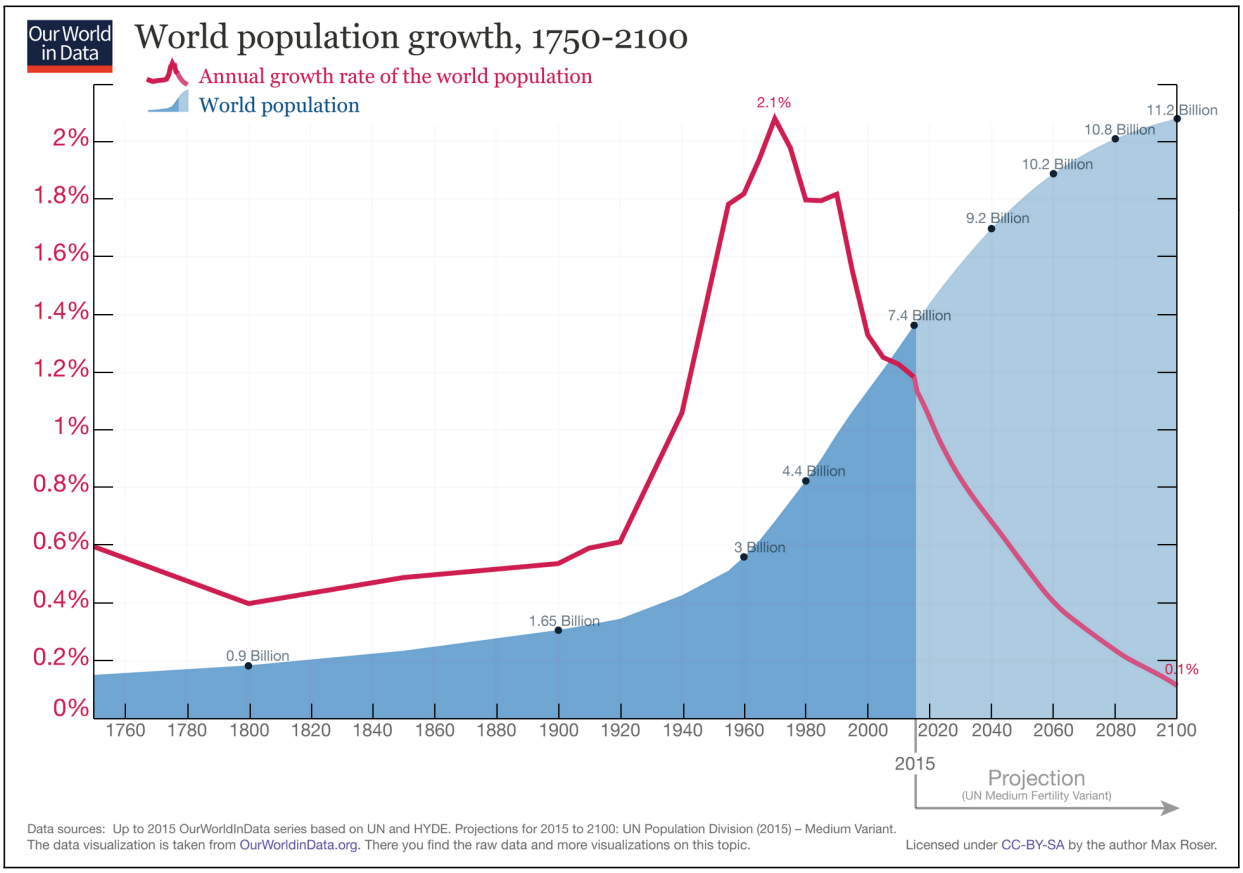

Fig. 8. World population growth. Plot from https://de.wikipedia.org/wiki/Datei:World-Population-Growth-1750-2100.png (Max Roser). Data from elaboration of data by United Nations, Department of Economic and Social Affairs, Population Division (63).

energies the growth 'constants' of the average consumption of fossil energies per person if we know how the growth 'constant' of the human population has been changing over time.

Fig. 8 illustrates this change of the growth constant k_1 of the human population since 1750 till now and predicts its further reduction after 2015 (66). It shows that the maximum growth constant k_1 of the human population occurred in 1969 at 2.1% per year and since then has been declining. Presently, it has been halved to about 1.0% since its peak in 1969. The amazing result from this analysis is that in 1969 the growth constant k_2 of the average use of fossil energies per person was only 0.4% per year, namely 2.5% minus 2.1%, which corresponds to a doubling time of 173 (ln2/0.4%) years. By contrast, the doubling time of the human population at that time was alarming and much shorter, namely merely 33 (ln2/2.1%) years. Today, the exponential growth constant k_1 of the human population has been reduced to 1.03% per year and hence its doubling time has doubled to 67 (ln2/1.03%) years, which is still much too short. However, the exponential growth constant k_2 of the average use of fossil energies per person has now risen to an alarming 1.47% per year, since it adds up with today's annual population growth constant k_1 of 1.03% (Fig. 8) to 2.5% per year (Fig. 5). Hence, the doubling time of the average use of fossil energies per person has been reduced to a mere 47 (ln2/1.47%) years and, on the basis of Figs. 5 and 8, is predicted to further decrease if excessive consumption of fossil energies continues as in the past. Thus, while the doubling time of the human population growth has been increasing steadily from 33 years in 1969 to 67 years now, the doubling time of the average consumption of fossil energies per person has been declining dramatically from 173 years in 1969 to 47 years today.

It seems surprising that the product of the human population and the average consumption of fossil energies per person increase exponentially with a constant growth constant k, as it is the sum of two apparently independent growth constants, that of the human population, k_1, and that of the average consumption of fossil energies per person, k_2, both of which reveal exponential growth with growth constants that change with time. Yet, it may appear more plausible if we consider the implication of this result: the smaller the population growth rate, the higher the average income per person and the higher the consumption of non-essential goods.

From all these considerations, it follows that it is important to reduce both the consumption of fossil energies per person and the growth of the human population. The general implications are clear. The richer a country, the faster it has to reduce its fossil energy consumption per person to zero whereas the contribution of poorer countries must consist primarily in their reduction of population growth to zero. Both aims have to be reached within the next 10 to 30 years (the shorter time for rich and developed countries, the longer for poor and developing countries) because the temperature anomaly is still increasing exponentially. As previously stated emphatically, this requires "a deep transformation (67) based on fundamental reorientation of human values, equity, behavior, institutions, economies, and technologies" (29).

Discussion

A crucial question we confront is whether the exponential rise in global temperature anomaly is caused by self-sustaining positive feedback mechanisms (discussed in ref. 68), as would be expected if a global tipping point, resulting from a cascade of local tipping points, is reached (27, 29–33, 69). If this occurs, the global temperature anomaly is no longer solely dependent on anthropogenic CO_2 emissions and hence can no longer be controlled (68–70). This study indicates that the current rise in global temperature anomaly is derived and not inherent, because it results from a similar rise in the accumulation of CO_2 emissions. The temperatures

that trigger local tipping points or a global tipping point are not known (71), but many climatologists suspect that several tipping points could be reached at temperatures 1.5°C to 2°C above pre-industrial temperatures (27, 29–31, 33, 72). These predictions are based on precedent.

Around 56 million years ago, the global temperature anomaly rose 5–8°C in 10,000 years and to 14°C above our measured pre-industrial temperature, sustaining elevated temperatures of the Paleocene–Eocene Thermal Maximum (PETM) for about 200,000 years (73–76). If we assume that the current rate of 0.29°C rise per decade remains constant, as would be the case if the anthropogenic emission remained constant at 36 Gt CO_2, the average global temperature would increase by 5–8°C in 170–270 years. This rate is 40–60 times faster than the maximum rate during PETM. Climate scientists predict that the global tipping point resulting in global catastrophe would be reached much earlier (27, 29–31, 33, 72, 77).

This fear is reinforced in several articles emphasizing that recent IPCC reports had focused on warming below 2°C (78) but had not explored whether or under which conditions climate change might threaten civilization (70, 77). As emphasized by Kemp et al. (70), the potential for catastrophic impacts depends decisively on the magnitude and rate of climate change. Therefore, it is crucial to be able to predict how the global temperature anomaly depends on anthropogenic CO_2 emission, and as demanded by prudent risk management, to consider bad-to-worst-case scenarios (70, 78–84).

As summarized in Table 1, my analysis demonstrates that if we continued to follow the trajectory pursued until 2015, the exponential rise of the global temperature anomaly, with a doubling time of 25.4±3.4 years (Fig. 2), would pass 3.2°C±1.1°C in 2050 and 14°C±7°C by the end of this century. This far exceeds the 4°C reached within the last two decades of this century considered by the IPCC (85) as well as its worst-case scenario, RCP 8.5 (86). Although during the past eight years, anthropogenic global CO_2 emissions rose at a constant rate of 35–37 Gt per year (Fig. 5 and Table 1), even the sum of these CO_2 emissions would not be enough to avoid a climate catastrophe (77). Importantly, the recent period of eight years of constant CO_2 emission has to be considered with caution, as it is not a statistically reliable deviation from exponential rise.

A constant CO_2 emission rate of 36 Gt is predicted to lead to a linear trajectory of the global temperature anomaly and to an increase of 2.1°C by 2050, 3.0°C by 2080, and 3.6°C by 2100. Consequently, if renewable energies (solar, wind, and geothermal) are substituted for fossil fuels and emissions of CO_2 and other greenhouse gases are curbed, the global temperature anomaly can stay below 2.1°C and worldwide climate neutrality can be reached by 2050. The trajectory to climate neutrality and the peak rise depend on the path we take.

The most ambitious pathway I considered results in a temperature limit of 1.6°C, while less ambitious scenarios result in global temperature anomalies of about 1.7°C. For example, reducing global CO_2 emission to zero in a linear fashion by 2050 will result in an accumulated emission of 774 Gt CO_2 since 2015[1], which corresponds to a global temperature anomaly of 1.73°C (Table 1). Alternatively, a linear reduction of emissions to 50% by the end of 2030 (50% is the goal as proposed by the USA in the Inflation Reduction Act (87) and of many climate activists), the accumulated CO_2 emission since 2015 will total 495 Gt[2], and result in a global temperature anomaly of 1.5°C (Table 1). In this scenario, we reach 1.5°C by 2030 while we have reduced annual global CO_2 emissions by only 50% to 18 Gt. Further

[1] Within the 27 years since the end of 2022, the accumulated CO_2 emission is 36 Gt x (27+26+...+1)/28 = 36/28 Gt x (27x28/2) = 36 Gt x 13.5 = 486 Gt CO_2. Adding the accumulated CO_2 emission between 2015 and the end of 2022, which is 288 Gt (Table 1), we obtain 486 Gt + 288 Gt = 774 Gt.

[2] This linear annual reduction of CO_2 emissions since the end of 2022 amounts to 36 Gt (15+14+...+9+8)/16 = 36/16 Gt x (15x16/2–7x8/2) = 36/16 x 92 Gt = 207 Gt, which corresponds to an accumulated CO_2 emission since 2015 of 207 Gt + 288 Gt = 495 Gt.

reducing global CO_2 emissions linearly to climate neutrality by 2050 adds an additional 171 Gt[3] and thus results in a total of 666 Gt in 2050 and a 1.64°C temperature rise (Table 1).

Given the current lack of consistent and unified worldwide efforts to reduce CO_2 emissions, it is more realistic to assume that CO_2 emissions will remain constant at 36 Gt until 2030 before a marked worldwide reduction will ensue. If we follow this path, we will reach an accumulated CO_2 emission of 540 Gt by the end of 2029, and a global temperature anomaly of 1.54°C (Table 1). If emissions are then reduced each year by 2 Gt, we will achieve climate neutrality by 2047. This scenario, with its average global temperature anomaly of 1.8°C (Table 1)[4], would have catastrophic consequences. The consequences of scenarios that achieve climate neutrality in 2060, 2070, 2080, or by the end of this century (with temperature anomalies that rise to 1.9°C, 2.0°C, 2.2°C, and 2.5°C, respectively) are far graver[5].

Some climate scientists argue that my analysis correlating the global temperature anomaly with anthropogenic CO_2 emission is too crude, as, in addition to atmospheric CO_2 concentration, many factors are known to affect global temperature. However, the striking correlation of its doubling time T_d of 25.4±3.4 years (Fig. 2) with those of the anthropogenic annual CO_2 emission (T_d = 27.5±1.6 years; Fig. 5), the atmospheric CO_2 concentration anomaly (T_d = 29.2±0.3 years; Fig. 4), and the accumulated CO_2 emission (T_d = 26.5±0.3 years; Fig. 6), all at a 95% confidence interval, support my analysis. It might indicate, at least as a first approximation, that (i) other factors contribute only little, (ii) largely compensate each other, and/or (iii) these factors also rise with a similar doubling time. For the greenhouse gas methane (i) and (iii) are indeed the case as its effect with respect to the rise of CO_2 in the atmosphere is still small and its lifetime within the atmosphere is negligible compared to that of CO_2. Finally, predictions from complex climate models have worsened several times during the past decade, suggesting that a different approach such as the one I propose merits consideration. I agree entirely with Kemp et al. (70) who conclude: "Facing a future of accelerating climate change while blind to worst-case scenarios is naive risk management at best and fatally foolish at worst."

Whether we will be successful in averting a climate catastrophe and environmental apocalypse (88, 89), decisively hinges on whether it is possible to change human consciousness (67). This cautiously gives me hope.

Acknowledgments

I thank Jacques Dubochet for discussions and pointing out that the exponential increase of CO_2 emissions can be explained by consumerism. I am especially indebted to John Sedat, Zvi Kam, and Peter Lawrence for comments and criticism of the manuscript. I thank Tom Kornberg for suggestions and diligent editing of the manuscript.

---

[3] In this case, the accumulated emission of CO_2 since 2030 is 18 Gt (19+18+...+2+1)/20 = 18 Gt x 9.5 = 171 Gt.

[4] In this scenario, an additional (34+32+30+ ... + 2) Gt = 2 Gt (1+2+...+17) = 17x18 Gt = 306 Gt CO_2 will accumulate since 2030, or 540 Gt + 306 Gt CO_2 = 846 Gt CO_2 since 2015, which corresponds to an average global temperature anomaly of 1.8°C (Table 1).

[5] Linear reduction of global CO_2 emissions to zero between the end of 2022 and the beginning of 2060 results in an accumulated CO_2 emission of 36 Gt (37+36+...+2+1)/38 = 666 Gt. Thus, the accumulated emission since 2015 is 954 Gt, which corresponds to a global temperature anomaly of 1.9°C (Table 1). Analogously, the accumulated emissions by 2070 and 280 are calculated to be (288 + 47x18) Gt = 1,134 Gt and (288 + 57x18) Gt = 1,314 Gt CO_2, respectively, corresponding to 2.0°C and 2.2°C. Analogously, should emissions be linearly reduced such that climate neutrality occurs only by the end of this century, the global temperature anomaly would rise to 2.5°C.

References

1. Stern SA. 1999. The lunar atmosphere: history, status, current problems, and context. Rev Geophys 37:453–491.
2. Vasavada AR, Paige DA, Wood SE. 1999. Near-surface temperatures on Mercury and the moon and the stability of polar ice deposits. Icarus 141:179–193.
3. Fourier J. 1824. Remarques générales sur les températures du globe terrestre et des espaces planétaires. Ann Chim Phys 27:136–167. 1896. Translated from the French: General remarks on the temperatures of the terrestrial globe and the planetary spaces. Am J Sci Arts 32:1–20.
4. Tyndall J. 1863. On radiation through the Earth's atmosphere. Phil Mag 25: 200–206.
5. Arrhenius S. 1896. On the influence of carbonic acid in the air upon the temperature of the ground. Phil Mag 41:237–276.
6. Foote E. 1856. Circumstances affecting the heat of the sun's rays. Am J Sci Arts 22:382–383.
7. Tyndall J. 1861. On the absorption and radiation of heat by gases and vapours, and on the physical connexion of radiation, absorption, and conduction. Phil Mag 22:169–194.
8. Hansen J, *et al*. 1981. Climate impact of increasing atmospheric carbon dioxide. Science 213:957–966.
9. Lacis AA, Schmidt GA, Rind D, Ruedy RA. 2010. Atmospheric CO_2: principal control knob governing Earth's temperature. Science 330:356–359.
10. Plass GN. 1956. The carbon dioxide theory of climatic change. Tellus 8:140–154.
11. Plass GN. 1956. Carbon dioxide and the climate. Am Scientist 44:302–316.
12. Callendar GS. 1938. The artificial production of carbon dioxide and its influence on temperature. Q J R Meteorol Soc 64:223–240.
13. Hawkins E, Jones PD. 2013. On increasing global temperatures: 75 years after Callendar. Q J R Meteorol Soc 139:1961–1963.
14. Bolin B, Eriksson E. 1959. Changes in the carbon dioxide content of the atmosphere and sea due to fossil fuel combustion. In: Bolin B, editor. The atmosphere and the sea in motion, Rossby Memorial Volume, New York: Rockefeller Institute Press. p. 130–142.
15. Revelle R, Suess HE. 1957. Carbon dioxide exchange between atmosphere and ocean and the question of an increase of atmospheric CO_2 during the past decades. Tellus 9:18–27.
16. Keeling CD. 1960. The concentration and isotopic abundances of carbon dioxide in the atmosphere. Tellus 12:200–203.
17. Keeling CD, *et al*. 1976. Atmospheric carbon dioxide variations at Mauna Loa Observatory, Hawaii. Tellus 28: 538–551.
18. Delmas RJ, Ascensio J-M, Legrand M. 1980. Polar ice evidence that atmospheric CO_2 20,000yr BP was 50% of present. Nature 284:155–157.
19. Jouzel J, *et al*. 1987. Vostok ice core: a continuous isotope temperature record over the last climatic cycle (160,000 years). Nature 329:403–408.
20. Barnola JM, Raynaud D, Korotkevich YS, Lorius C. 1987. Vostok ice core provides 160,000-year record of atmospheric CO_2. Nature 329:408–414.
21. Genthon G, *et al*. 1987. Vostok ice core: climatic response to CO_2 and orbital forcing changes over the last climatic cycle. Nature 329:414–418.
22. Petit JR, *et al*. 1999. Climate and atmospheric history of the past 420,000 years from the Vostok ice core, Antarctica. Nature 399:429–436.
23. Siegenthaler U, *et al*. 2005. Stable carbon cycle–climate relationship during the late Pleistocene. Science 310:1313–1317.

24. Lüthi DF, *et al*. 2008. High-resolution carbon dioxide concentration record 650,000–800,000 years before present. Nature 453:379–382.
25. Walter KM, Zimov SA, Chanton JP, Verbyla D, Chapin FS III. 2006. Methane bubbling from Siberian thaw lakes as a positive feedback to climate warming. Nature 443:71–75.
26. Brouillette M. 2021. The buried carbon bomb. Nature 591:360–362.
27. Lenton TM, *et al*. 2019. Climate tipping points – too risky to bet against. Nature 575:592–595.
28. Budyko MI. 1969. The effect of solar radiation variations on the climate of the Earth. Tellus 21:611–619.
29. Steffen W, *et al*. 2018. Trajectories of the earth system in the anthropocene. Proc Natl Acad Sci USA 115:8252–8259.
30. Schellnhuber HJ, Rahmstorf S, Winkelmann R. 2016. Why the right climate target was agreed in Paris. Nature Clim Change 6:649–653.
31. Lenton TM, *et al*. 2008. Tipping elements in the Earth's climate system. Proc Natl Acad Sci USA 105:1786–1793.
32. Rocha JC, Peterson G, Bodin Ö, Levin S. 2018. Cascading regime shifts within and across scales. Science 362:1379–1383.
33. Wunderling N, Donges JF, Kurths J, Winkelmann R. 2021. Interacting tipping elements increase risk of climate domino effects under global warming. Earth Syst Dynam 12:601–619.
34. Ross SM. 2014. Introduction to Probability and Statistics for Engineers and Scientists, Chapter 9: Regression. 5th ed. San Diego: Academic Press.
35. https://en.wikipedia.org/wiki/Regression_analysis
36. https://en.wikipedia.org/wiki/Least_squares
37. http://www.real-statistics.com/correlation/basic-concepts-correlation/
38. https://en.wikipedia.org/wiki/Pearson_correlation_coefficient
39. https://en.wikipedia.org/wiki/Coefficient_of_determination
40. Hansen J, *et al*. 1988. Global climate changes as forecast by Goddard Institute for Space Studies three-dimensional model. J Geophys Res 93:9341–9364.
41. Hansen J, Ruedy R, Sato M, Lo K. 2010. Global surface temperature change. Rev Geophys 48:RG4004. Update: https://data.giss.nasa.gov/gistemp/graphs_v4/ under 'Global Annual Mean Surface Air Temperature Change'.
42. Meadows DH, Meadows DL, Randers J, Behrens WW. 1972. The Limits to Growth. A Report for the Club of Rome's Project on the Predicament of Mankind. New York: Universe Books.
43. https://www.sealevel.info/co2_and_ch4.html
44. Hays JD, Imbrie J, Shackleton NJ. 1976. Variations in the Earth's orbit: pacemaker of the ice ages. Science 194:1121–1132.
45. Shackleton NG. 2000. The 100,000-year ice-age cycle identified and found to lag temperature, carbon dioxide and orbital eccentricity. Science 289:1897–1902.
46. Sawyer JS. 1972. Man-made carbon dioxide and the "greenhouse" effect. Nature 239:23–26.
47. Meadows D, Randers J, Meadows D. 2004. Limits to Growth, The 30-Year Update. White River Junction, Vermont: Chelsea Green Publishing Company.
48. Manabe S, Wetherald RT. 1967. Thermal equilibrium of the atmosphere with a given distribution of relative humidity. J Atmos Sci 24:241–259.
49. Hegerl GC, Crowley TJ, Hyde WT, Frame DJ. 2006. Climate sensitivity constrained by temperature reconstructions over the past seven centuries. Nature 440:1029–1032.
50. Cox PM, Huntingford C, Williamson MS. 2018. Emergent constraint on equilibrium climate sensitivity from global temperature variability. Nature 553:319–322.

51. Pan Y, *et al*. 2011. A large and persistent carbon sink in the world's forests. Science 333:988–993.
52. Baccini A, *et al*. 2017. Tropical forests are a net carbon source based on aboveground measurements of gain and loss. Science 358:230–234.
53. Walker XJ, *et al*. 2019. Increasing wildfires threaten historic carbon sink of boreal forest soils. Nature 572:520–523.
54. Gatti LV, *et al*. 2021. Amazonia as a carbon source linked to deforestation and climate change. Nature 595:388–393.
55. Cox PM, *et al*. 2008. Increasing risk of Amazonian drought due to decreasing aerosol pollution. Nature 453:212–215.
56. Gruber N, *et al*. 2019. The oceanic sink for anthropogenic CO_2 from 1994 to 2007. Science 363:1193–1199.
57. https://cdiac.ess-dive.lbl.gov/ftp/ndp030/global.1751_2014.ems
58. Figueres C, *et al.* 2017. Three years to safeguard our climate. Nature 546:593–595.
59. Irwin R. 2017. Progress, exponential growth and post-growth education. Educational Studies in Japan: International Yearbook 11:57–70.
60. Allen MR, *et al*. 2009. Warming caused by cumulative carbon emissions towards the trillionth tonne. Nature 458:1163–1166.
61. Matthews HD, Gillett NP, Stott PA, Zickfeld K. 2009. The proportionality of global warming to cumulative carbon emissions. Nature 459:829–832.
62. https://www.unep.org/news-and-stories/press-release/cut-global-emissions-76-percent-every-year-next-decade-meet-15degc
63. https://report.ipcc.ch/ar6wg3/pdf/IPCC_AR6_WGIII_SummaryForPolicymakers.pdf
64. https://www.ipcc.ch/sr15/chapter/chapter-2/
65. Meinshausen M, *et al*. 2022. Realization of Paris agreement pledges may limit warming just below 2°C. Nature 604:304–309.
66. https://www.worldometers.info/world-population/world-population-by-year/
67. Hardin G. 1968. The tragedy of the commons. Science 162:1243–1248.
68. Kareiva P, Carranza V. 2018. Essential risk due to ecosystem collapse: Nature strikes back. Futures 102:39–50.
69. Klose AK, Wunderling N, Winkelmann R, Donges JF. 2021. What do we mean, 'tipping cascade'? Environ Res Lett 16:125011.
70. Kemp L, *et al*. 2022. Climate endgame: exploring catastrophic climate change scenarios. Proc Natl Acad Sci USA 119 (34):e2108146119.
71. Kriegler E, Hall JW, Held H, Dawson R, Schellnhuber HJ. 2009. Imprecise probability assessment of tipping points in the climate system. Proc Natl Acad Sci USA 106: 5041–5046.
72. Armstrong McKay DI, *et al*. 2022. Exceeding 1.5°C global warming could trigger multiple climate tipping points. Science 377:eabn7950.
73. McInerny FA, Wing SL. 2011. The Paleocene–Eocene Thermal Maximum: a perturbation of carbon cycle, climatre, and biosphere with implications for the future. Annu Rev Earth Planet Sci 39:489–516.
74. Burke KD, *et al*. 2018. Pliocene and Eocene provide best analogs for near-future climates. Proc Natl Acad Sci USA 115:13288–13293.
75. Haynes LL, Hönisch B. 2020. The seawater carbon inventory at the Paleocene–Eocene Thermal Maximum. Proc Natl Acad Sci USA 117: 24088–24095.
76. Tierney JE, *et al*. 2022. Spatial patterns of climate change across the Paleocene–Eocene Thermal Maximum. Proc Natl Acad Sci USA 119 (42):e2205326119.
77. Steel D, DesRoches CT, Mintz-Woo K. 2022. Climate change and the threat to civilization. Proc Natl Acad Sci USA 119 (42):e2210525119.

78. Jehn FU, *et al*. 2022. Focus of the IPCC assessment reports has shifted to lower temperatures. Earth's Future 10:e2022EF002876.
79. Beard SJ, *et al*. 2021. Assessing climate change's contribution to global catastrophic risk. Futures 127, 102673.
80. Weitzman ML. 2011. Fat-tailed uncertainty in the economics of catastrophic climate change. Rev Environ Econ Policy 5:275–292.
81. Richards CE, Lupton RC, Allwood JM. 2021. Re-framing the threat of global warming: an empirical causal loop diagram of climate change, food insecurity and societal collapse. Clim Change 164:49.
82. Dietz S. 2011. High impact, low probability? An empirical analysis of risk in the economics of climate change. Clim Change 108:519–541.
83. Kunreuther H, *et al*. 2013. Risk management and climate change. Nature Clim Change 3:447–450.
84. Dittrich R, Wreford A, Moran D. 2016. A survey of decision-making approaches for climate change adaptation: Are robust methods the way foreward? Ecol Econ 122:79–89.
85. IPCC, *Climate change 2021*: *The physical science basis. Contribution of working group I to the sixth assessment report of the intergovernmental panel on climate change*, V. Masson-Delmotte *et al*., Eds. (Cambridge University Press, Cambridge, UK and New York, NY, 2021). https://www.ipcc.ch/report/ar6/wg1/downloads/report/IPCC_AR6_WGI_FullReport.pdf.
86. Schwalm CR, Glendon S, Duffy PB. 2020. RCP8.5 tracks cumulative CO_2 emissions. Proc Natl Acad Sci USA 117:19656–19657.
87. https://en.wikipedia.org/wiki/Inflation_Reduction_Act_of_2022
88. Rockström J, *et al*. 2009. A safe operating space for humanity. Nature 461:472–475.
89. Barnosky AD, *et al*. 2011. Has the Earth's sixth mass extinction already arrived? Nature 471:51–57.